

A catalog of 171 high-quality binary black-hole simulations for gravitational-wave astronomy

Abdul H. Mroué,¹ Mark A. Scheel,² Béla Szilágyi,² Harald P. Pfeiffer,^{1,3} Michael Boyle,⁴ Daniel A. Hemberger,⁴ Lawrence E. Kidder,⁴ Geoffrey Lovelace,^{5,2} Serguei Ossokine,^{1,6} Nicholas W. Taylor,² Anil Zenginoğlu,² Luisa T. Buchman,² Tony Chu,¹ Evan Foley,⁵ Matthew Giesler,⁵ Robert Owen,⁷ and Saul A. Teukolsky⁴

¹Canadian Institute for Theoretical Astrophysics, 60 St. George Street, University of Toronto, Toronto, ON M5S 3H8, Canada

²Theoretical Astrophysics 350-17, California Institute of Technology, Pasadena, CA 91125, USA

³Canadian Institute for Advanced Research, 180 Dundas St. West, Toronto, ON M5G 1Z8, Canada

⁴Center for Radiophysics and Space Research, Cornell University, Ithaca, New York 14853, USA

⁵Gravitational Wave Physics and Astronomy Center, California State University Fullerton, Fullerton, California 92834, USA

⁶Department of Astronomy and Astrophysics, 50 St. George Street, University of Toronto, Toronto, ON M5S 3H4, Canada

⁷Department of Physics and Astronomy, Oberlin College, Oberlin, Ohio 44074, USA

(Dated: June 4, 2013)

Coalescing binary black holes are a primary science target of ground-based gravitational-wave detectors. Detecting gravitational waves from these binaries and understanding the properties of the waves' sources require detailed knowledge of the expected waveforms. This paper presents a catalog of numerical binary black-hole simulations that represents a major advance toward the application of numerical relativity to gravitational-wave data analysis. The 171 simulations in the catalog include 90 precessing binaries, mass ratios up to 8:1, orbital eccentricities from a few percent to 10^{-5} , and black-hole spins up to 97% of the theoretical maximum. The simulations follow more orbits (up to 34) than previous simulations, allowing a more reliable connection to approximate analytical waveforms, which are used to extend numerical waveforms to span the entire frequency range of a detector. The expanded parameter-space coverage of this catalog, together with the length and accuracy of the included waveforms, will facilitate the development of new (and improvement of existing) gravitational-wave template families, the study of detection efficiency of gravitational-wave searches, and the understanding of systematic biases in parameter estimation of detected gravitational waves. Formidable challenges remain; for example, precession complicates the connection of numerical and approximate analytical waveforms, and vast regions of the parameter space remain unexplored.

PACS numbers: 04.25.D-, 04.25.dg, 04.30.-w, 04.30.Db

INTRODUCTION

Gravitational waves (GW) from coalescing compact-object binaries — neutron stars (NS) and stellar-mass black holes (BH) — are primary targets for the next generation of GW detectors, such as Advanced LIGO, Virgo and KAGRA [1–4]. Detecting GWs from compact-object binaries requires high-quality, accurate theoretical waveform models for GW template banks. Similarly, measuring source properties of detected signals (“parameter estimation”) relies on theoretical waveform models used in Markov Chain Monte Carlo algorithms [5].

For widely separated binaries, post-Newtonian (PN) calculations [6] provide gravitational waveforms to good accuracy. However, numerical simulations of the full Einstein equations are needed for the late inspiral, merger, and ringdown portions of the binary evolution. Such simulations are particularly important for stellar-mass BH-BH and BH-NS systems: Late inspiral and merger occur near LIGO’s most sensitive frequency range, and although BHs might have high spins [7, 8], some of the spin contributions to the PN waveforms are known only to lower expansion order than the non-spinning terms [9–32].

This paper focuses on binary black holes (BBH). Numerical simulations of BBHs became possible eight years ago [33], with tremendous progress since (e.g., [34, 35]). For best utility to GW astronomy, such simulations must satisfy several conditions: (i) sufficient accuracy; (ii) astrophysical relevance, particularly low orbital eccentricity [36, 37]; (iii) sufficient length (i.e., number of orbits) to connect reliably to PN waveforms; (iv) sufficiently dense coverage of relevant regions of parameter space.

The precise requirements for these conditions are application dependent. For instance, 10 orbits is sufficient for GW *detection* at BBH parameters that are straightforward to simulate (mass ratio $q \lesssim 4$, dimensionless spins $\chi \equiv S/M^2 \lesssim 0.7$ aligned with the orbital angular momentum) [38]. On the other hand, *parameter estimation* can benefit from well over 100 orbits [38–41]. Requirements become more stringent with more extreme BH spin and mass ratio [40]. For precessing binaries, analogous studies have not even been performed because of a lack of inspiral-merger-ringdown waveform models.

Satisfying all conditions (i) to (iv) is so difficult that, despite advances in numerical methods, simulations have barely reached the minimal desired quality. For instance, the world-wide NINJA-2 collaboration [42] resulted in 40

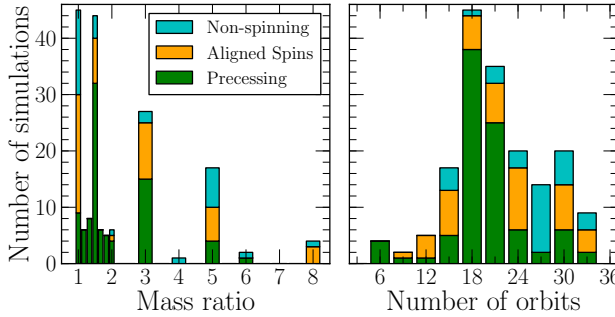


FIG. 1. Number of simulations vs. mass ratio and number of orbits. We separately list non-spinning, aligned-spin and precessing BBH systems.

waveforms with an average length of ~ 9 orbits, essentially covering only two one-dimensional subspaces of the aligned spin region of the parameter space. The NR-AR collaboration [43, 44] is collecting and evaluating the accuracy of a smaller number of waveforms from systems with somewhat more general parameters than NINJA-2. A recent study [45] reports about 80 simulations covering approximately 7–12 orbits (~ 25 of them representing precessing binaries) and ~ 170 simulations lasting a few orbits each.

This paper represents a major advance in waveform length and parameter-space coverage. We follow our earlier approach [46–49] of computing black-hole simulations of the highest quality: longer than previous simulations, with higher accuracy and very low eccentricity. Our catalog contains 171 simulations, with almost all covering more than 12 orbits and the longest covering 34 orbits (Fig. 1). 90 simulations represent precessing binaries.

The remainder of this paper summarizes our computational techniques, describes the catalog, and discusses applications and challenges for future work.

TECHNIQUES

The simulations described here are computed using the Spectral Einstein Code (**SpEC**) [50]. This multi-domain pseudospectral code includes an elliptic solver [51] and a hyperbolic evolution module [46–48, 52–58] to construct initial data and evolve it.

Initial data are constructed [59, 60] to satisfy the Einstein constraint equations with two black holes in quasi-equilibrium [61–65]. Initial separation depends on the desired length of the inspiral, whereas the orbital frequency and the radial velocities of the black holes are determined iteratively [66, 67] to achieve eccentricities of $\sim 10^{-4}$.

SpEC employs singularity excision using a computational domain extending from excision boundaries just inside each apparent horizon to some large radius of or-

der several hundred M , where M is the total mass of the system. (Here $G=c=1$, so that time, length, and mass have the same dimensions.) Our first-order representation [53] of the generalized harmonic formulation [68–70] of Einstein’s equations enables us to choose pure-outflow excision boundaries, which need no boundary conditions.

Our outer boundary conditions [53, 71, 72] reduce the influx of constraint violations [73–79] and undesired incoming gravitational radiation [80, 81]. Running simulations through merger robustly requires damped harmonic gauge conditions [55, 82, 83], grids conforming to the shapes of the horizons [48, 55, 57, 58], and adaptive mesh refinement [56]. After a common apparent horizon forms, the evolution is continued on a new computational domain with a single excision boundary lying just inside the common apparent horizon and conforming to the common horizon’s shape [48, 57].

Gravitational radiation is extracted from the simulations by two independent methods: the Newman-Penrose curvature scalar Ψ_4 as described in [49, 64] and the Regge-Wheeler-Zerilli (RWZ) gravitational wave strain $h_{\ell m}$ [84–86]. These waveforms, extracted at a series of finite-radius coordinate spheres, are extrapolated to infinite distance from the source using techniques developed in [87] with modifications suggested in [88] to account for precession.

CATALOG

The catalog is summarized in Fig. 2. Simulations 0001–0065 correspond to initial-data set \mathcal{S}_0 from [67]. Most of these simulations have BH spins of either 0 or 0.5, oriented in different directions. Simulations 0066–0114 evolve several mass and spin configurations at multiple eccentricities between 10^{-4} and ~ 0.06 . Simulations 0115–0146 correspond to initial-data set \mathcal{S}_5 from [67]; they have random mass ratios in the range $1 \leq q \leq 2$, random spin directions, and random spin magnitudes in the range $0 \leq \chi \leq 0.5$. Simulation 0147 is a super-kick [89–91] configuration, with anti-parallel black hole spins tangential to the orbital plane.

Simulations 0148–0165 use superposed Kerr-Schild initial data [65, 92], which enable BH spins larger than $\chi \approx 0.93$, a bound that arises from other initial data constructions [65, 93]. Simulations 0149–0160 represent a sequence of equal-mass, equal-spin configurations with spins parallel or anti-parallel to the orbital angular momentum (presented in more detail in [94]).

Simulations 0166–0171 represent unequal-mass non-spinning simulations and equal-mass, equal aligned spin simulations already published in [46, 95, 96]. The first published inspiral-merger-ringdown **SpEC** simulation (an equal-mass, zero-spin BBH [48] lasting about $4000M$) is not included in the catalog, because we did not output enough information to apply our present extrapolation.

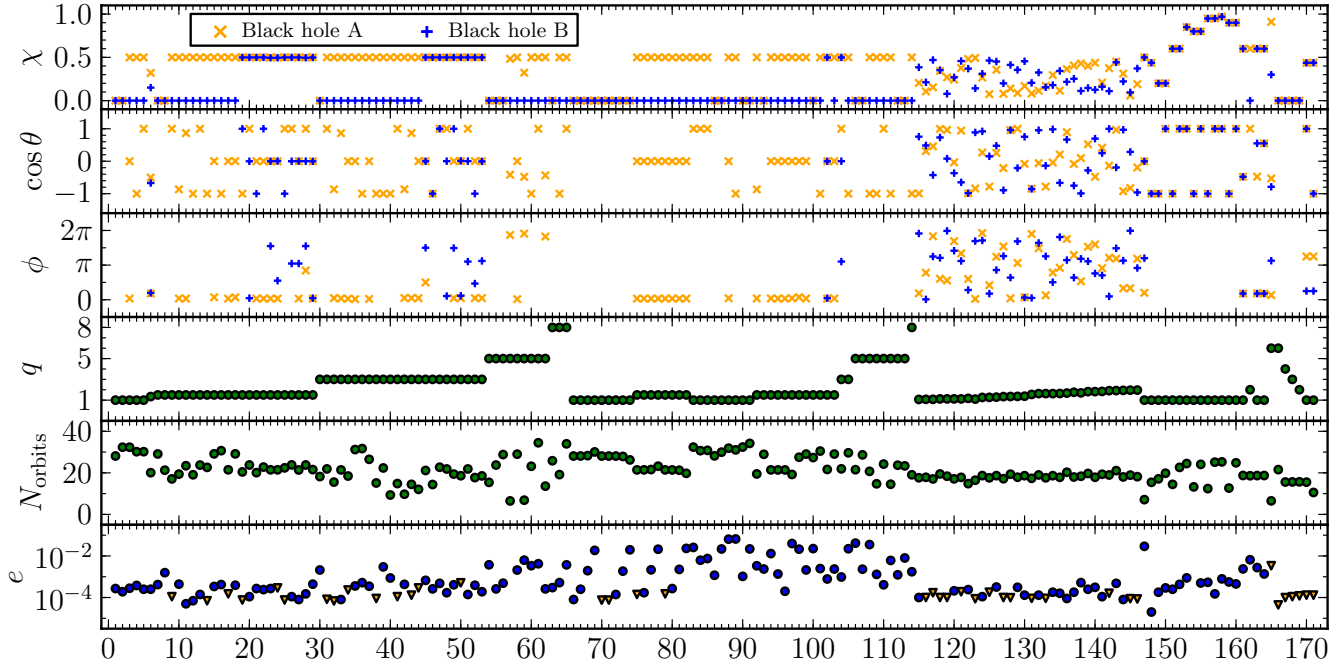


FIG. 2. Properties of all simulations in the catalog. From top to bottom: dimensionless initial spin magnitudes $\chi_{A,B}$; angles $\theta_{A,B}$ between the initial spin vectors and the initial orbital angular momentum; angles $\phi_{A,B}$ between the line segment connecting the centers of the black holes and the initial spin vectors projected into the initial orbital plane; mass ratio $q = M_A/M_B$; number of orbits before merger; initial eccentricity e (triangles indicate an upper bound on e).

tion techniques; however, improved equal-mass, zero-spin simulations are included (0001 and 0002).

Figure 3 plots the gravitational-wave polarizations h_+ and h_\times emitted into a certain sky direction, chosen such that h_\times vanishes for non-precessing systems.

Figure 4 highlights two precessing systems. (i) Simulation 0035 is a $q = 3$ precessing configuration following 31 orbits. This simulation proceeds through about 1.5 precession cycles: the normal to the instantaneous orbital plane traces out the orange precession cone with opening angle 35° , whereas the BH spin of the more massive black hole traces out a precession cone with an opening angle of 144° . (ii) Simulation 0165 is a $q = 6$ configuration with both black holes spinning in generic directions, and spin magnitudes $\chi_A = 0.9$, $\chi_B = 0.3$. The orbital plane changes by almost 90° , and the spin direction of the smaller black hole traces out a spiral motion.

Figure 5 shows the waveforms for simulation 0035 in two sky directions, highlighting the strong dependence of the waveforms on the orientation of the BBH relative to the line of sight to Earth. This figure also presents a convergence test, showing differences in the waveforms computed using different numerical resolutions. These differences decrease rapidly with increasing resolution, illustrating the exponential convergence provided by spectral numerical methods. Compared to our previous equal-mass non-spinning simulation [48, 49] and the unequal-mass non-spinning simulations [46] (all instrumental for

various GW data-analysis applications [42, 85, 97, 98]), 0035 achieves a smaller cumulative phase error (0.07 rad) even though it is three times longer. Out of the 171 simulations in the catalog, 57 (36) simulations were repeated for at least two (three) resolutions. We estimate the accuracy of configurations with only one resolution by comparing with nearby configurations in the parameter space; a more detailed discussion of the accuracy of waveforms in our catalog will be presented in [99].

DISCUSSION

This paper presents the most comprehensive catalog of high-quality BBH simulations to date, enabling studies to help maximize the impact of GW detectors and to increase our understanding of GW sources and dynamical, strongly curved spacetime:

Accuracy of PN precession equations: PN theory predicts how spin and orbital angular momenta precess in generic binaries [9, 10, 15, 16, 19–21, 23, 25, 27, 29, 31, 100–102]. The simulations here are long enough for detailed comparisons at different points in parameter space. Accurate modeling of precession dynamics is also expected to be a key step toward constructing precessing waveform models [103].

PN accuracy studies, extended to a larger region of parameter space and to an earlier stage of the inspiral: Pre-

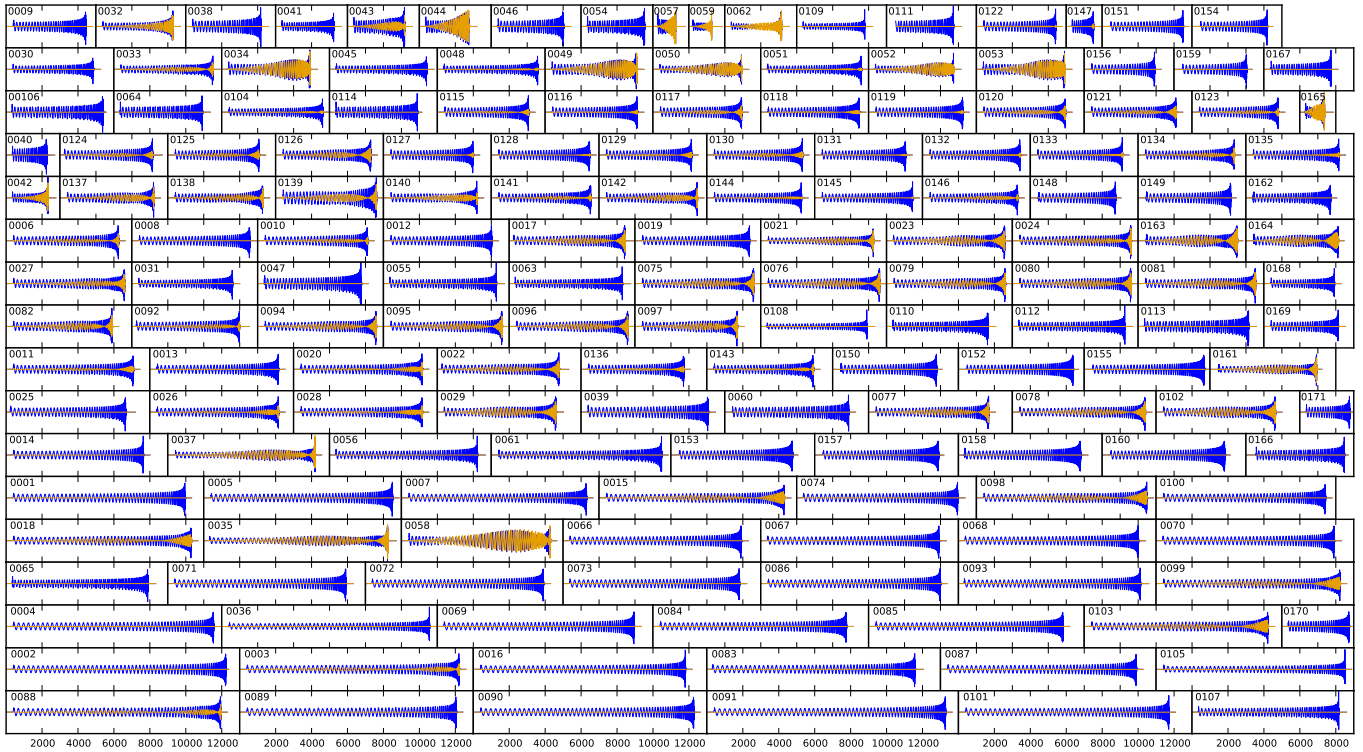


FIG. 3. Waveform polarizations h_+ (blue) and h_x (orange) in a sky direction parallel to the initial orbital plane of each simulation. All plots have the same horizontal scale, with each tick representing a time interval of $2000M$ (equal to 0.2 s for a $20M_\odot$ BBH).

vious studies consider only aligned spins [47, 104, 105] and at best either 15–20 orbits [39, 49] or a few orbits at very large separation [106]. With the longer waveforms in this catalog, these studies can extend to the earlier part of the inspiral, where PN theory is expected to be more accurate, and to include a larger region of parameter space.

Independent validation of existing analytical waveform models: Many waveform models [86, 107–111] are calibrated against numerical relativity simulations—but usually only with a small number of simulations, which are comparatively short (typically < 10 orbits). The new simulations here enable tests of these models at different points in parameter space and covering more cycles.

Detection sensitivity: Following the approach taken in the NINJA projects [42, 98, 112], our waveforms can be injected into GW detector noise to study the efficiency of GW data-analysis pipelines. Injections of precessing and/or eccentric waveforms from this catalog can quantify the impact of precession and eccentricity on the detection sensitivity of current searches using circular, aligned-spin templates. The new waveforms will also help assess the performance of searches with precessing waveform templates.

Systematic errors in parameter estimation: Parameter estimation methods [5] currently use inspiral-only PN waveforms. Applying parameter estimation methods to

the waveforms in this catalog will enable the systematic errors of this approach to be quantified.

Construction of precessing inspiral-merger-ringdown waveform models: This catalog will enable the construction of sophisticated phenomenological or effective-one-body waveform models for precessing binaries, extending the first such effort [113].

Periastron advance can be studied in aligned spin binaries and generic binaries [114, 115].

While this catalog will enable pioneering studies, major challenges remain for future work. First, for a waveform to be most useful for data analysis, it must be connected to a PN waveform from the early inspiral, forming a *hybrid waveform* [42] that spans the entire frequency range of a GW detector. This is difficult for precessing configurations, because of both the complexity of precessing PN waveforms and ambiguities in connecting PN binary parameters with the numerical binary parameters [88].

Second, most of the parameter space remains unexplored. Only 24 configurations have mass ratio $q > 3$ (cf. Fig. 1); of these, only 5 are precessing, and almost none have a spinning smaller black hole. Spinning BBH systems for $5 \lesssim q \lesssim 10$ are particularly interesting because they serve as accurate proxies for BH-NS binaries. Furthermore, the catalog contains only three simulations (the only three to date [47, 94]) with spins $\chi \geq 0.93$ (i.e.,

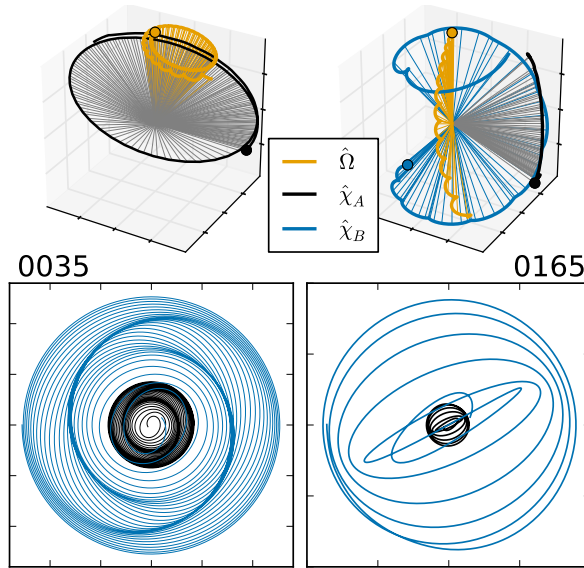


FIG. 4. Precessing simulations 0035 and 0165. **Top:** Precession cones traced by the orbital angular momentum and the spin vectors of the BHs. The circles denote the initial location of the vectors. For 0035 (left), $\chi_B = 0$. **Bottom:** Trajectories of the individual black holes, projected into the initial orbital plane.

above the “Bowen-York limit” [116–120].

Finally, some of the simulations here utilize several algorithmic improvements, most notably adaptive mesh refinement (AMR) to dynamically adjust the number of pseudospectral collocation points. AMR achieves high accuracy but complicates convergence tests; therefore, some simulations do not display convergence properties as clearly as in Fig. 5. This will be discussed within a more comprehensive analysis of this catalog in a forthcoming publication [99]. Instructions for how to access, understand, and interpret the catalog will be provided in [99].

We thank Christian Ott and Kip Thorne for helpful discussions. This work was supported by NSERC of Canada, the Canada Chairs Program, and the Canadian Institute for Advanced Research; the Sherman Fairchild Foundation; NSF grants PHY-0969111 and PHY-1005426 at Cornell, and NSF grants PHY-1068881, PHY-1005655, and DMS-1065438 at Caltech. Simulations used in this work were computed with the `SpEC` code [50]. Computations were performed on the Zwicky cluster at Caltech, which is supported by the Sherman Fairchild Foundation and by NSF award PHY-0960291; on the NSF XSEDE network under grant TG-PHY990007N; and on the GPC supercomputer at the SciNet HPC Consortium [121]. SciNet is funded by: the Canada Foundation for Innovation under the auspices of Compute Canada; the Government of Ontario; Ontario Research Fund–Research Excellence; and the University of Toronto.

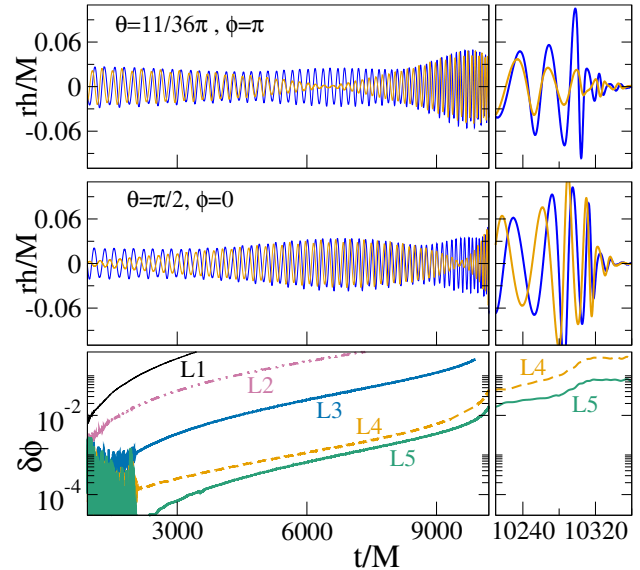


FIG. 5. Waveforms and a convergence test for configuration 0035. **Top, middle:** waveforms h_+ (blue) and h_x (orange) for two different angles (θ, ϕ) of the detector relative to the initial orbital angular momentum. The left panels show the inspiral and the right panels show the merger on an expanded horizontal scale. **Bottom:** cumulative phase differences between the dominant $\ell = 2, m = 2$ spherical-harmonic mode of the waveform of a given numerical resolution (labeled L1 through L5 in order of increasing resolution) compared to that of the highest resolution L6. The plot excludes the early part of the waveform where initial transients are present.

- [1] G. M. Harry (LIGO Scientific Collaboration), *Class. Quant. Grav.* **27**, 084006 (2010).
- [2] The Virgo Collaboration, “Advanced Virgo Baseline Design,” (2009), [VIR-0027A-09].
- [3] The Virgo Collaboration, “Advanced Virgo Technical Design Report,” (2012), [VIR-0128A-12].
- [4] K. Somiya and the KAGRA Collaboration, *Class. Quantum Grav.* **29**, 124007 (2012).
- [5] J. Aasi *et al.* (the LIGO Scientific Collaboration, the Virgo Collaboration), (2013), arXiv:1304.1775 [gr-qc].
- [6] L. Blanchet, *Living Rev. Rel.* **9**, 4 (2006).
- [7] L. Gou, J. E. McClintock, M. J. Reid, J. A. Orosz, J. F. Steiner, R. Narayan, J. Xiang, R. A. Remillard, K. A. Arnaud, and S. W. Davis, *Astrophys. J.* **742**, 85 (2011), arXiv:1106.3690 [astro-ph.HE].
- [8] J. E. McClintock, R. Shafee, R. Narayan, R. A. Remillard, S. W. Davis, and L.-X. Li, *Astrophys. J.* **652**, 518 (2006).
- [9] B. M. Barker and R. F. O’Connell, *Phys. Rev.* **D12**, 329 (1975).
- [10] B. M. Barker and R. F. O’Connell, *General Relativity and Gravitation* **11**, 149 (1979).
- [11] L. E. Kidder, C. M. Will, and A. G. Wiseman, *Phys. Rev. D* **47**, 4183 (1993), arXiv:gr-qc/9211025.
- [12] T. A. Apostolatos, C. Cutler, G. J. Sussman, and K. S. Thorne, *Phys. Rev. D* **49**, 6274 (1994).

[13] L. E. Kidder, Phys. Rev. D **52**, 821 (1995).

[14] B. J. Owen, H. Tagoshi, and A. Ohashi, Phys. Rev. D **57**, 6168 (1998), arXiv:gr-qc/9710134.

[15] H. Tagoshi, A. Ohashi, and B. J. Owen, Phys. Rev. D **63**, 044006 (2001).

[16] R. A. Porto, Phys. Rev. D **73**, 104031 (2006), arXiv:gr-qc/0511061 [gr-qc].

[17] R. A. Porto and I. Z. Rothstein, Phys. Rev. Lett. **97**, 021101 (2006), arXiv:gr-qc/0604099 [gr-qc].

[18] L. Blanchet, A. Buonanno, and G. Faye, Phys. Rev. D **74**, 104034 (2006).

[19] T. Damour, P. Jaranowski, and G. Schaefer, Phys. Rev. D **77**, 064032 (2008), arXiv:0711.1048 [gr-qc].

[20] R. A. Porto and I. Z. Rothstein, Phys. Rev. D **78**, 044013 (2008), arXiv:0804.0260 [gr-qc].

[21] R. A. Porto and I. Z. Rothstein, Phys. Rev. D **78**, 044012 (2008), arXiv:0802.0720 [gr-qc].

[22] J. Steinhoff, S. Hergt, and G. Schäfer, Phys. Rev. D **78**, 101503 (2008), arXiv:0809.2200 [gr-qc].

[23] M. Levi, Phys. Rev. D **82**, 104004 (2010), arXiv:1006.4139 [gr-qc].

[24] R. A. Porto, A. Ross, and I. Z. Rothstein, JCAP **1103**, 009 (2011), arXiv:1007.1312 [gr-qc].

[25] R. A. Porto, Class. Quant. Grav. **27**, 205001 (2010), arXiv:1005.5730 [gr-qc].

[26] L. Blanchet, A. Buonanno, and G. Faye, Phys. Rev. D **84**, 064041 (2011), arXiv:1104.5659 [gr-qc].

[27] S. Hergt, J. Steinhoff, and G. Schäfer, Classical and Quantum Gravity **27**, 135007 (2010), arXiv:1002.2093 [gr-qc].

[28] J. Hartung and J. Steinhoff, Annalen der Physik **523**, 783 (2011), arXiv:1104.3079 [gr-qc].

[29] J. Hartung and J. Steinhoff, Annalen der Physik **523**, 919 (2011), arXiv:1107.4294 [gr-qc].

[30] R. A. Porto, A. Ross, and I. Z. Rothstein, JCAP **1209**, 028 (2012), arXiv:1203.2962 [gr-qc].

[31] J. Hartung, J. Steinhoff, and G. Schäfer, ArXiv e-prints (2013), arXiv:1302.6723 [gr-qc].

[32] A. Bohe, S. Marsat, and L. Blanchet, ArXiv e-prints (2013), arXiv:1303.7412 [gr-qc].

[33] F. Pretorius, Phys. Rev. Lett. **95**, 121101 (2005), arXiv:gr-qc/0507014 [gr-qc].

[34] J. Centrella, J. G. Baker, B. J. Kelly, and J. R. van Meter, Rev. Mod. Phys. **82**, 3069 (2010).

[35] H. P. Pfeiffer, Class. Quant. Grav. **29**, 124004 (2012), arXiv:1203.5166 [gr-qc].

[36] P. C. Peters and J. Mathews, Phys. Rev. **131**, 435 (1963).

[37] P. C. Peters, Phys. Rev. **136**, B1224 (1964).

[38] F. Ohme, M. Hannam, and S. Husa, Phys. Rev. D **84**, 064029 (2011).

[39] I. MacDonald, A. H. Mroué, H. P. Pfeiffer, M. Boyle, L. E. Kidder, M. A. Scheel, B. Szilágyi, and N. W. Taylor, Phys. Rev. D **87**, 024009 (2013), arXiv:1210.3007 [gr-qc].

[40] M. Boyle, Phys. Rev. D **84**, 064013 (2011).

[41] T. Damour, A. Nagar, and M. Trias, Phys. Rev. D **83**, 024006 (2011), arXiv:1009.5998 [gr-qc].

[42] P. Ajith, M. Boyle, D. A. Brown, B. Brugmann, L. T. Buchman, *et al.*, Class. Quantum Grav. **29**, 124001 (2012).

[43] The Numerical Relativity and Analytical Relativity (NRAR) collaboration.

[44] I. Hinder *et al.*, “First results from the Numerical-Relativity–Analytical-Relativity collaboration,” (2013), in preparation.

[45] L. Pekowsky, R. O’Shaughnessy, J. Healy, and D. Shoemaker, (2013), arXiv:1304.3176 [gr-qc].

[46] L. T. Buchman, H. P. Pfeiffer, M. A. Scheel, and B. Szilágyi, Phys. Rev. D **86**, 084033 (2012), arXiv:1206.3015 [gr-qc].

[47] G. Lovelace, M. Boyle, M. A. Scheel, and B. Szilágyi, Class. Quant. Grav. **29**, 045003 (2012), arXiv:arXiv:1110.2229 [gr-qc].

[48] M. A. Scheel, M. Boyle, T. Chu, L. E. Kidder, K. D. Matthews and H. P. Pfeiffer, Phys. Rev. D **79**, 024003 (2009), arXiv:gr-qc/0810.1767.

[49] M. Boyle, D. A. Brown, L. E. Kidder, A. H. Mroué, H. P. Pfeiffer, M. A. Scheel, G. B. Cook, and S. A. Teukolsky, Phys. Rev. D **76**, 124038 (2007).

[50] <http://www.black-holes.org/SpEC.html>.

[51] H. P. Pfeiffer, L. E. Kidder, M. A. Scheel, and S. A. Teukolsky, Comput. Phys. Commun. **152**, 253 (2003).

[52] L. E. Kidder, M. A. Scheel, S. A. Teukolsky, E. D. Carlson, and G. B. Cook, Phys. Rev. D **62**, 084032 (2000).

[53] L. Lindblom, M. A. Scheel, L. E. Kidder, R. Owen, and O. Rinne, Class. Quantum Grav. **23**, S447 (2006).

[54] M. A. Scheel, H. P. Pfeiffer, L. Lindblom, L. E. Kidder, O. Rinne, and S. A. Teukolsky, Phys. Rev. D **74**, 104006 (2006).

[55] B. Szilágyi, L. Lindblom, and M. A. Scheel, Phys. Rev. D **80**, 124010 (2009), arXiv:0909.3557 [gr-qc].

[56] G. Lovelace, M. A. Scheel, and B. Szilágyi, Phys. Rev. D **83**, 024010 (2011), arXiv:1010.2777 [gr-qc].

[57] D. A. Hemberger, M. A. Scheel, L. E. Kidder, B. Szilágyi, and S. A. Teukolsky, Class. Quantum Grav. **30**, 115001 (2013), arXiv:1211.6079 [gr-qc].

[58] S. Ossokine, L. E. Kidder, and H. P. Pfeiffer, (2013), arXiv:1304.3067 [gr-qc].

[59] J. W. York, Phys. Rev. Lett. **82**, 1350 (1999).

[60] H. P. Pfeiffer and J. W. York, Phys. Rev. D **67**, 044022 (2003).

[61] G. B. Cook, Phys. Rev. D **65**, 084003 (2002).

[62] G. B. Cook and H. P. Pfeiffer, Phys. Rev. D **70**, 104016 (2004).

[63] M. Caudill, G. B. Cook, J. D. Grigsby, and H. P. Pfeiffer, Phys. Rev. D **74**, 064011 (2006), gr-qc/0605053.

[64] H. P. Pfeiffer, D. A. Brown, L. E. Kidder, L. Lindblom, G. Lovelace, and M. A. Scheel, Class. Quantum Grav. **24**, S59 (2007), gr-qc/0702106.

[65] G. Lovelace, R. Owen, H. P. Pfeiffer, and T. Chu, Phys. Rev. D **78**, 084017 (2008).

[66] A. Buonanno, L. E. Kidder, A. H. Mroué, H. P. Pfeiffer, and A. Taracchini, Phys. Rev. D **83**, 104034 (2011), arXiv:1012.1549 [gr-qc].

[67] A. H. Mroué and H. P. Pfeiffer, (2012), arXiv:1210.2958 [gr-qc].

[68] H. Friedrich, Commun. Math. Phys. **100**, 525 (1985).

[69] D. Garfinkle, Phys. Rev. D **65**, 044029 (2002).

[70] F. Pretorius, Class. Quantum Grav. **22**, 425 (2005).

[71] O. Rinne, Class. Quantum Grav. **23**, 6275 (2006).

[72] O. Rinne, L. Lindblom, and M. A. Scheel, Class. Quantum Grav. **24**, 4053 (2007).

[73] J. M. Stewart, Class. Quantum Grav. **15**, 2865 (1998).

[74] H. Friedrich and G. Nagy, Commun. Math. Phys. **201**, 619 (1999).

[75] J. M. Bardeen and L. T. Buchman, Phys. Rev. D **65**, 064037 (2002).

[76] B. Szilágyi, B. Schmidt, and J. Winicour, Phys. Rev. D **65**, 064015 (2002).

[77] G. Calabrese, J. Pullin, O. Reula, O. Sarbach, and M. Tiglio, Commun. Math. Phys. **240**, 377 (2003), gr-qc/0209017.

[78] B. Szilágyi and J. Winicour, Phys. Rev. D **68**, 041501(R) (2003).

[79] L. E. Kidder, L. Lindblom, M. A. Scheel, L. T. Buchman, and H. P. Pfeiffer, Phys. Rev. D **71**, 064020 (2005).

[80] L. T. Buchman and O. C. A. Sarbach, Class. Quantum Grav. **23**, 6709 (2006).

[81] L. T. Buchman and O. C. A. Sarbach, Class. Quantum Grav. **24**, S307 (2007).

[82] L. Lindblom and B. Szilágyi, Phys. Rev. D **80**, 084019 (2009), arXiv:0904.4873.

[83] M. W. Choptuik and F. Pretorius, Phys. Rev. Lett. **104**, 111101 (2010), arXiv:0908.1780 [gr-qc].

[84] O. Rinne, L. T. Buchman, M. A. Scheel, and H. P. Pfeiffer, Class. Quantum Grav. **26**, 075009 (2009).

[85] Y. Pan, A. Buonanno, M. Boyle, L. T. Buchman, L. E. Kidder, H. P. Pfeiffer, and M. A. Scheel, Phys. Rev. D **84**, 124052 (2011), arXiv:1106.1021 [gr-qc].

[86] A. Buonanno, Y. Pan, H. P. Pfeiffer, M. A. Scheel, L. T. Buchman, and L. E. Kidder, Phys. Rev. D **79**, 124028 (2009), arXiv:0902.0790 [gr-qc].

[87] M. Boyle and A. H. Mroué, Phys. Rev. D **80**, 124045 (2009), arXiv:0905.3177 [gr-qc].

[88] M. Boyle, “Angular velocity of gravitational radiation from precessing binaries and the corotating frame,” (2013), accepted for publication in Phys. Rev. D, arXiv:1302.2919 [gr-qc].

[89] M. Campanelli, C. O. Lousto, Y. Zlochower, and D. Merritt, Phys. Rev. Lett. **98**, 231102 (2007), gr-qc/0702133.

[90] B. Brügmann, J. A. González, M. Hannam, S. Husa, and U. Sperhake, Phys. Rev. D **77**, 124047 (2008), arXiv:arXiv:0707.0135 [gr-qc].

[91] C. O. Lousto and Y. Zlochower, Phys. Rev. Lett. **107**, 231102 (2011), arXiv:1108.2009 [gr-qc].

[92] P. Marronetti and R. A. Matzner, Phys. Rev. Lett. **85**, 5500 (2000).

[93] S. Dain, C. O. Lousto, and Y. Zlochower, Phys. Rev. D **78**, 024039 (2008), arXiv:0803.0351v2 [gr-qc].

[94] D. A. Hemberger, G. Lovelace, T. J. Loredo, L. E. Kidder, S. A. Teukolsky, and M. Giesler, In prep. (2013).

[95] T. Chu, *Numerical simulations of black-hole spacetimes*, Ph.D. thesis, California Institute of Technology (2012).

[96] T. Chu, H. P. Pfeiffer, and M. A. Scheel, Phys. Rev. D **80**, 124051 (2009), arXiv:0909.1313 [gr-qc].

[97] Y. Pan, A. Buonanno, M. Boyle, L. T. Buchman, L. E. Kidder, *et al.*, Phys. Rev. D **84**, 124052 (2011), arXiv:1106.1021 [gr-qc].

[98] B. Aylott, J. G. Baker, W. D. Boggs, M. Boyle, P. R. Brady, *et al.*, Class.Quant.Grav. **26**, 165008 (2009), arXiv:0901.4399 [gr-qc].

[99] A. Mroué, M. Scheel, B. Szilagyi, H. Pfeiffer, M. Boyle, D. Hemberger, L. Kidder, G. Lovelace, S. Ossokine, N. Taylor, A. Zenginoglu, L. Buchman, T. Chu, E. Foley, M. Giesler, R. Owen, and S. Teukolsky, (In Prep.).

[100] K. S. Thorne and J. B. Hartle, Phys. Rev. D **31**, 1815 (1985).

[101] G. Faye, L. Blanchet, and A. Buonanno, Phys. Rev. D **74**, 104033 (2006).

[102] M. Levi, (2011), arXiv:1107.4322 [gr-qc].

[103] P. Schmidt, M. Hannam, and S. Husa, (2012), arXiv:1207.3088 [gr-qc].

[104] M. Hannam, S. Husa, F. Ohme, D. Muller, and B. Bruegmann, Phys. Rev. D **82**, 124008 (2010), arXiv:1007.4789 [gr-qc].

[105] M. Hannam, S. Husa, B. Brügmann, and A. Gopakumar, Phys. Rev. D **78**, 104007 (2008).

[106] C. O. Lousto and Y. Zlochower, (2013), arXiv:1304.3937 [gr-qc].

[107] T. Damour, A. Nagar, M. Hannam, S. Husa, and B. Bruegmann, Phys. Rev. D **78**, 044039 (2008), arXiv:0803.3162 [gr-qc].

[108] P. Ajith, M. Hannam, S. Husa, Y. Chen, B. Bruegmann, N. Dorband, D. Mueller, F. Ohme, D. Pollney, C. Reisswig, L. Santamaria, and J. Seiler, (2009), arXiv:0909.2867 [gr-qc].

[109] Y. Pan, A. Buonanno, L. T. Buchman, T. Chu, L. E. Kidder, H. P. Pfeiffer, and M. A. Scheel, Phys. Rev. D **81**, 084041 (2010), arXiv:0912.3466 [gr-qc].

[110] L. Santamaría, F. Ohme, P. Ajith, B. Brügmann, N. Dorband, M. Hannam, S. Husa, P. Mösta, D. Pollney, C. Reisswig, E. L. Robinson, J. Seiler, and B. Krishnan, Phys. Rev. D **82**, 064016 (2010), arXiv:1005.3306 [gr-qc].

[111] A. Taracchini, Y. Pan, A. Buonanno, E. Barausse, M. Boyle, T. Chu, G. Lovelace, H. P. Pfeiffer, and M. A. Scheel, Phys. Rev. D **83**, 104034 (2012), arXiv:1202.0790 [gr-qc].

[112] B. Aylott *et al.*, Class. Quant. Grav. **26**, 114008 (2009), arXiv:0905.4227 [gr-qc].

[113] R. Sturani, S. Fischetti, L. Cadonati, G. Guidi, J. Healy, *et al.*, J.Phys.Conf.Ser. **243**, 012007 (2010), arXiv:1005.0551 [gr-qc].

[114] A. Le Tiec, A. H. Mroué, L. Barak, A. Buonanno, H. P. Pfeiffer, N. Sago, and A. Taracchini, Phys. Rev. Lett. **107**, 141101 (2011), arXiv:1106.3278 [gr-qc].

[115] A. H. Mroué, H. P. Pfeiffer, L. E. Kidder, and S. A. Teukolsky, Phys. Rev. D **82**, 124016 (2010), arXiv:1004.4697 [gr-qc].

[116] J. M. Bowen, Gen. Relativ. Gravit. **11**, 227 (1979).

[117] J. M. Bowen and J. W. York, Jr., Phys. Rev. D **21**, 2047 (1980).

[118] G. B. Cook and J. W. York, Jr., Phys. Rev. D **41**, 1077 (1990).

[119] S. Dain, C. O. Lousto, and R. Takahashi, Phys. Rev. D **65**, 104038 (2002).

[120] M. Hannam, S. Husa, and N. O. Murchadha, Phys. Rev. D **80**, 124007 (2009).

[121] C. Loken, D. Gruner, L. Groer, R. Peltier, N. Bunn, M. Craig, T. Henriques, J. Dempsey, C.-H. Yu, J. Chen, L. J. Dursi, J. Chong, S. Northrup, J. Pinto, N. Knecht, and R. V. Zon, J. Phys.: Conf. Ser. **256**, 012026 (2010).